Applied Physics Letters

RESEARCH ARTICLE | NOVEMBER 05 2020

Spin–orbit torques in structures with asymmetric dusting layers

Special Collection: Spin-Orbit Torque (SOT): Materials, Physics, and Devices

Armin Razavi ; Hao Wu; Bingqian Dai; Haoran He; Di Wu; Kin Wong ; Guoqiang Yu ; Kang L. Wang

Appl. Phys. Lett. 117, 182403 (2020)
https://doi.org/10.1063/5.0029347

Applied Physics Letters ARTICLE scitation.org/journal/apl

Spin–orbit torques in structures with asymmetric dusting layers

Cite as: Appl. Phys. Lett. **117**, 182403 (2020); doi: 10.1063/5.0029347
Submitted: 11 September 2020 · Accepted: 25 October 2020 ·
Published Online: 5 November 2020

Armin Razavi,[1] Hao Wu,[1] Bingqian Dai,[1] Haoran He,[1] Di Wu,[1] Kin Wong,[1] Guoqiang Yu,[2] and Kang L. Wang[1,a)]

AFFILIATIONS

[1]Department of Electrical and Computer Engineering, University of California, Los Angeles, California 90095, USA
[2]Beijing National Laboratory for Condensed Matter Physics, Institute of Physics, Chinese Academy of Sciences, Beijing 100190, China

Note: This paper is part of the Special Topic on Spin-Orbit Torque (SOT): Materials, Physics and Devices.
[a)]**Author to whom correspondence should be addressed:** wang@ee.ucla.edu

ABSTRACT

Current-induced spin–orbit torques (SOTs) in heavy metal/ferromagnet heterostructures have emerged as an efficient method for magnetization switching with applications in nonvolatile magnetic memory and logic devices. However, experimental realization of SOT switching of perpendicular magnetization requires an additional inversion symmetry breaking, calling for modifications of the conventional SOT heterostructures. In this work, we study SOTs and deterministic switching of perpendicular magnetization by inserting different asymmetric dusting layers at the heavy metal/ferromagnet interface. Similar to the previous works with lateral structural asymmetry, we study the emergence of current-induced perpendicular effective magnetic fields (H_z^{eff}). By examining three different material combinations of heavy metal/dusting layers (W/IrMn, Pt/IrMn, and W/Ta), we shed light on the origins of H_z^{eff}; we show that H_z^{eff} is generically created in all the studied asymmetric structures, has a close correlation with the interfacial magnetic anisotropy, and is independent of the signs of spin Hall angles of the materials. Furthermore, we show that the induction of H_z^{eff} enables field-free deterministic SOT switching of perpendicular magnetization. Our results can be used in designing SOT heterostructures for practical applications in nonvolatile technologies.

Spintronic devices provide an attractive platform for implementing fast, energy-efficient, high-density, and nonvolatile memory and logic devices. In these devices, information is stored in the magnetization state of a free magnetic layer, and electrical means are utilized for magnetization manipulation. One promising method for magnetization switching is based on the current-induced spin–orbit torques (SOTs),[1–3] with faster dynamics, higher endurance, and potentially higher energy efficiency compared with the conventional spin-transfer torque.[4–7] The emergence of SOTs depends on a combination of high spin–orbit coupling and inversion symmetry breaking; consequently, SOT heterostructures mainly consist of a heavy-metal/ferromagnet bilayer. Applying an in-plane current in such structures results in the damping-like and field-like SOTs, which can be mostly attributed to the spin Hall[8–10] and Rashba–Edelstein effects,[11,12] although not limited to them.[13–17] Heterostructures with perpendicular magnetic anisotropy (PMA) are most desirable for practical applications, since they give rise to a higher device density and a lower switching current density compared to the materials with in-plane magnetic anisotropy.[18,19] However, SOT switching of perpendicular magnetization requires an additional inversion symmetry breaking, which has typically been achieved by applying an external magnetic field collinear with the current, making it impractical for applications. As a consequence, there has been plenty of effort recently to realize deterministic switching of perpendicular magnetization without external fields, including the use of lateral structural asymmetry,[20–25] an in-plane exchange bias field,[26–29] chiral symmetry breaking,[30] and competing spin currents,[31] among other methods.[32–37]

In this work, we use the concept of lateral structural asymmetry[20] and modify the conventional SOT heterostructure by inserting a second asymmetric dusting heavy-metal layer at the main heavy-metal/ferromagnet interface. By breaking the structure's symmetry in the in-plane lateral direction (transverse to the charge current direction), it has been shown that current-induced perpendicular effective SOT magnetic fields (H_z^{eff}) can be created, resulting in the field-free switching of perpendicular magnetization. In the previous works, the use of asymmetric oxide,[20,24] ferromagnets,[22] heavy metals,[25] and thin light metal insertion[23] has been explored. Here, we study the insertion of different asymmetric heavy metal dusting layers in three representative material systems of (W/IrMn, Pt/IrMn, and W/Ta)/CoFeB/MgO, where the second layer in each sample is the asymmetric dusting

insertion. The studied structures in this work are quite similar to the ones with an asymmetric *light metal* insertion;[23] however, here we study the insertion of *heavy metal* dusting layers. The presence of two heavy metals in our heterostructures allows us to compare our results with the earlier report on competing spin currents[31] and shed light on the origins of H_z^{eff} in such material systems. We show that H_z^{eff} can be generically created in all the asymmetric structures, has a correlation with interfacial magnetic anisotropy, and is independent of the signs of the spin Hall angles, in stark contrast to the previous report.[31] We also realize deterministic field-free switching of perpendicular magnetization by using the induced H_z^{eff}.

The samples were deposited on thermally oxidized Si (001) substrates by a magnetron sputtering system at room temperature via an oblique angle deposition. For the layers with uniform thickness, the substrates were rotated during the deposition. For the asymmetric wedge-shaped layers, we stopped the substrate rotation during the deposition. The heterostructures consist of the core multilayers of heavy metal/asymmetric dusting insertion/ferromagnet/oxide, as shown in Fig. 1(a). We study three different material systems: (i) W(5)/IrMn(0.5-w)/CoFeB(0.9)/MgO(2)/Ta(2), (ii) Ta(2)/Pt(5)/IrMn(1.0-w)/CoFeB(0.9)/MgO(2)/Ta(2), and (iii) W(5)/Ta(0.5-w)/CoFeB(0.9)/MgO(2)/Ta(2), which we will refer to as W/IrMn, Pt/IrMn, and W/Ta, respectively. Here, the numbers in parentheses represent thicknesses in nm, and w indicates the wedge shape of the layer. The number attached to w shows the wedge layer's thickness at the center of the sample's length. The 0.5 w and 1.0 w wedge layers yield an average nominal thickness gradient of 77 pm and 155 pm per cm of the sample length, respectively. In a previous work, we have shown the uniformity and high interface quality of such samples (W/IrMn) using high resolution transmission electron microscopy (HR-TEM).[38] For samples (i)–(iii), W, Pt, and W serve as the main heavy metal layer, respectively. The bottom and top Ta(2) in all these samples serve as either buffer or capping layers. We should note that the IrMn layers used here are very thin and have a Néel temperature much below the room temperature, and so these layers do not have any antiferromagnetic properties. The multilayer stacks were patterned into standard Hall bars (a length of 130 μm and a width of 20 μm) by using photolithography combined with dry etching, as shown in Fig. 1(c). Cr(10)/Au(100) metal stacks were deposited as electrodes. All the measurements were carried out at room temperature.

In conventional SOT heterostructures, all the layers have uniform thicknesses and the inversion symmetry is only broken along the perpendicular z axis, resulting in the field-like and damping-like SOTs which are proportional to $\gamma H_y^{FL} \boldsymbol{m} \times \hat{y}$ and $\gamma H_x^{DL} \boldsymbol{m} \times \boldsymbol{m} \times \hat{y}$, respectively, where γ and $\boldsymbol{m}$ are the gyromagnetic ratio and unit vector of magnetization.[39] However, in our heterostructures, the inversion symmetry is also broken along the y axis, i.e., we are breaking the mirror symmetry with respect to the x-z plane, as shown in Fig. 1(b). As a

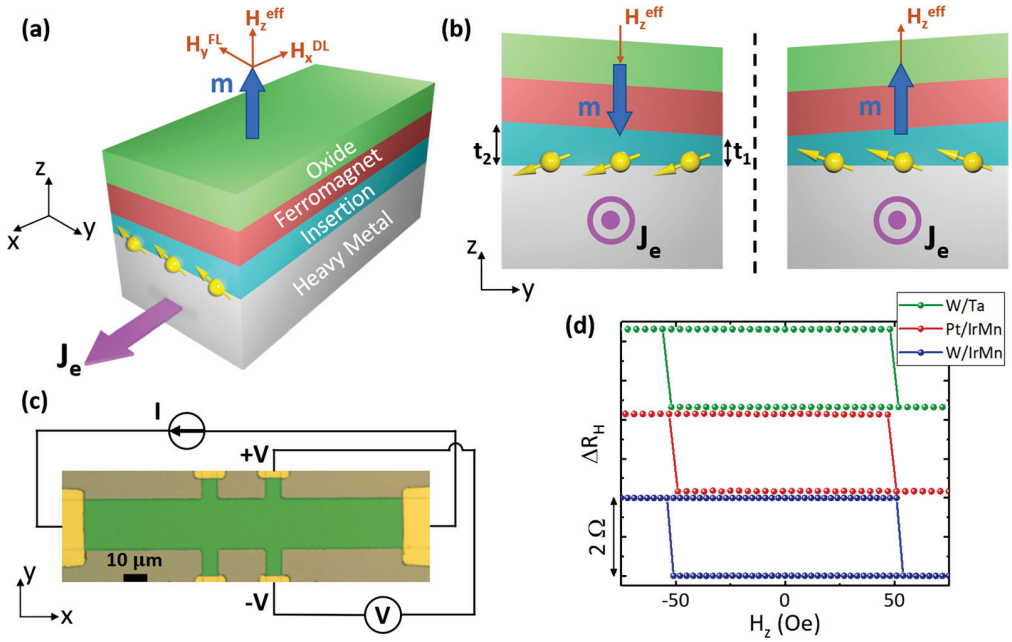

FIG. 1. Breaking the lateral structural symmetry by a thin wedge-shaped dusting layer insertion. (a) A schematic of the studied SOT heterostructures. The insertion layer has a wedge shape and breaks the structural symmetry, resulting in the creation of current-induced out-of-plane effective SOT magnetic fields (H_z^{eff}). H_x^{DL} and H_y^{FL} denote the conventional damping-like and field-like SOTs, respectively. $\mathbf{J_e}$ is the charge current density and **m** is the unit vector of magnetization. The yellow spheres with arrows represent the created effective net spin polarization. (b) The cross section of the studied structure, and its mirror image with respect to the x-z plane. The dusting layer has a small thickness gradient; hence, it has different thicknesses t_1 and t_2 at the two ends of the device, and it breaks the mirror symmetry with respect to the x-z plane. As an example, charge current applied in $\pm\hat{x}$ direction creates H_z^{eff} pointing in $\mp\hat{z}$. (c) Hall bar structures and the transport measurement configurations. I and V are the applied current and measured Hall voltage, respectively. (d) Perpendicular magnetic anisotropy and coercivity of the three different samples. R_H and H_z denote the anomalous Hall resistance and external perpendicular magnetic field, respectively. All these devices are picked from the center of the three samples, with insertion layer thicknesses of 0.5 and 1.0 nm. The applied current density is around 9×10^9 A/m^2.

result, out-of-plane current-induced effective magnetic fields H_z^{eff} are expected from the symmetry arguments.[20] We can see the emergence of H_z^{eff} by examining the Rashba spin–orbit coupling Hamiltonian $H_R = \frac{\alpha_R}{\hbar}\boldsymbol{\sigma} \cdot (\boldsymbol{E} \times \boldsymbol{p})$.[11,12] Here, α_R, $\hbar$, $\boldsymbol{\sigma}$, $\boldsymbol{E}$, and $\boldsymbol{p}$ denote the Rashba parameter, reduced Plank constant, Pauli matrices, effective electric field, and electron momentum, respectively. By breaking the mirror symmetry with respect to the x-z plane, microscopic effective electric fields along the y axis are allowed, and when the charge current is applied along the x axis, an effective perpendicular magnetic field (H_z^{eff}) can be induced. Microscopically, in addition to the Rashba–Edelstein effect,[20,23] the induction of H_z^{eff} can potentially be explained by a gradient of magnetic anisotropy and chiral symmetry breaking,[30] and other interfacial effects arising from the added in-plane asymmetry,[13,14] all of which would require the lateral structural symmetry breaking. We should note that in our devices, the thickness gradient of dusting layers is extremely small; the average nominal thickness difference between the two edges of our Hall bars [t_2-t_1 in Fig. 1(b)] is less than 1 pm. However, we still have an effective symmetry breaking in our samples, which might be due to a tilted deposition direction away from the substrate's normal, resulting from oblique angle deposition without substrate rotation.[23,25] Consequently, the symmetry breaking might arise from a possible tilt of the polycrystalline texture[40] and not the thickness difference across a device.

We use the anomalous Hall effect to characterize our devices, with current applied along the x axis and Hall voltage measured along the y axis, as shown in Fig. 1(c). All the studied samples have perpendicular anisotropy, as the sharp switching with an applied perpendicular field in Fig. 1(d) suggests. For characterizing H_z^{eff}, we perform the anomalous Hall measurements with opposite polarities of the applied current and examine the hysteresis loop shifts from the center.[20] Figure 2(a) shows such shifted loops for the W/IrMn sample. The value of shifts for each current density corresponds to the opposite of H_z^{eff}. It should be noted that the reduced coercivities compared to Fig. 1(d) are a result of the Joule heating effect.

We observe a linear relationship between the applied current density and H_z^{eff} in all the devices, as shown in Fig. 2(b). We define β

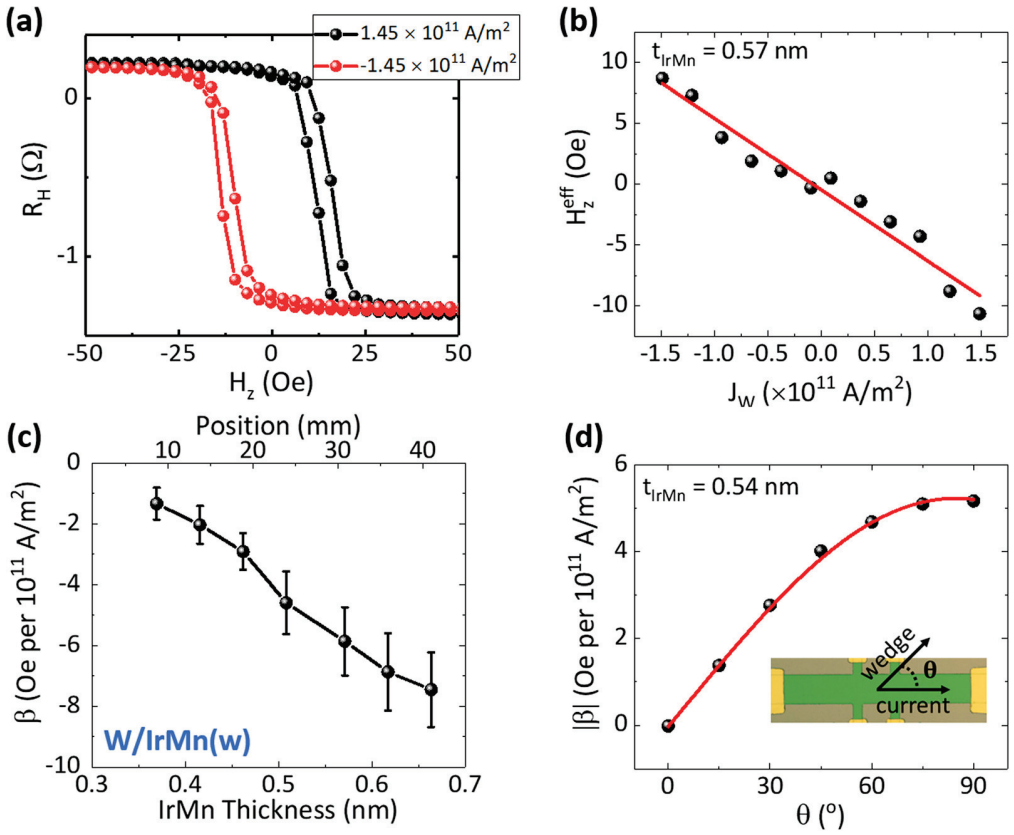

FIG. 2. Characterization of current-induced out-of-plane effective fields H_z^{eff} using the anomalous Hall effect for the W/IrMn sample. (a) Out-of-plane hysteresis loops are shifted to opposite directions for opposite current polarities. The current densities are estimated for the W layer based on the conductivities of different layers. The nominal IrMn insertion thickness in this device is 0.61 nm. R_H and H_z denote the anomalous Hall resistance and the applied perpendicular field. (b) A linear relationship is observed between H_z^{eff} and the applied current density through the W layer (J_W). The red linear fitting shows the slope β. The IrMn insertion thickness for this device is 0.57 nm. (c) Plot of β as a function of the IrMn insertion thickness (and the device position on the sample). The error bars are obtained from averaging three different devices and considering the linear fitting errors. The negative sign of β shows that for a current applied in the $+\hat{x}$ direction, H_z^{eff} points in the $-\hat{z}$ direction. (d) Angular dependence of $|\beta|$. θ is defined as the angle between the current and wedge directions, as shown in the inset. The IrMn insertion thickness for this device is 0.54 nm. The red line shows a sin θ fit to the data points.

as the slope ($\frac{\partial H_z^{eff}}{\partial J}$) and plot it as a function of the IrMn insertion thickness and device position in Fig. 2(c). β is strongly modulated by small changes in the IrMn thickness; its magnitude changes by more than a factor of 4 when the IrMn thickness changes from 0.35 to 0.65 nm. We find relatively close agreement between the PMA gradient and β as a function of the IrMn thickness (see Fig. S1 in the supplementary material). This observation points to the possible role of chiral symmetry breaking in the creation of H_z^{eff},[30] where a larger gradient of magnetic anisotropy results in a larger H_z^{eff} (see supplementary material Sec. S2 for a discussion of the chiral symmetry breaking). Furthermore, such a correlation between the interfacial anisotropy gradient and β in Fig. S1 points to the possible interfacial origin of H_z^{eff} in this system, rather than a bulk origin. To confirm the importance of lateral structural asymmetry in our samples, we fabricated a series of devices with different angles between the current and wedge directions (θ) and studied β as a function of this angle, as shown in Fig. 2(d). H_z^{eff} requires perpendicular wedge and current directions; consequently, it has a sin θ angular dependence, as generically observed in previous works as well.[20,23] We should add that no H_z^{eff} is observed in samples with uniform layers (see Fig. S3 in the supplementary material).

For the W/IrMn/CoFeB/MgO sample, the materials W and IrMn have opposite signs of the spin Hall angle.[41] It has been proposed that in such structures with double heavy metals, an opposite sign of the spin Hall angles is required for the creation of H_z^{eff} (the competing spin current requirement).[31] However, we also observed the creation of H_z^{eff} in the Pt/IrMn/CoFeB/MgO system, in which Pt and IrMn have the same sign of the spin Hall angle, in stark contrast to the previous report on competing spin currents.[31] By applying currents with opposite polarities, we observe that out-of-plane hysteresis loops are shifted in opposite directions (see Fig. S4 in the supplementary material). We also obtained the β values as a function of the IrMn insertion thickness, as shown in Fig. 3(a). These results suggest that the creation of H_z^{eff} is independent of the relative signs of the spin Hall angles of the two heavy metals. We also observe that β undergoes a sign change at around 0.8–0.9 nm of IrMn thickness. To find out the reason for this behavior, we looked at the trends of conventional SOTs and the PMA gradient with the IrMn thickness.

Figure 3(b) shows the extracted effective SOT fields as a function of the IrMn insertion thickness (see supplementary material Sec. S5 for more details). Here, we have averaged the absolute values of effective fields for down/up magnetizations for a clear representation.

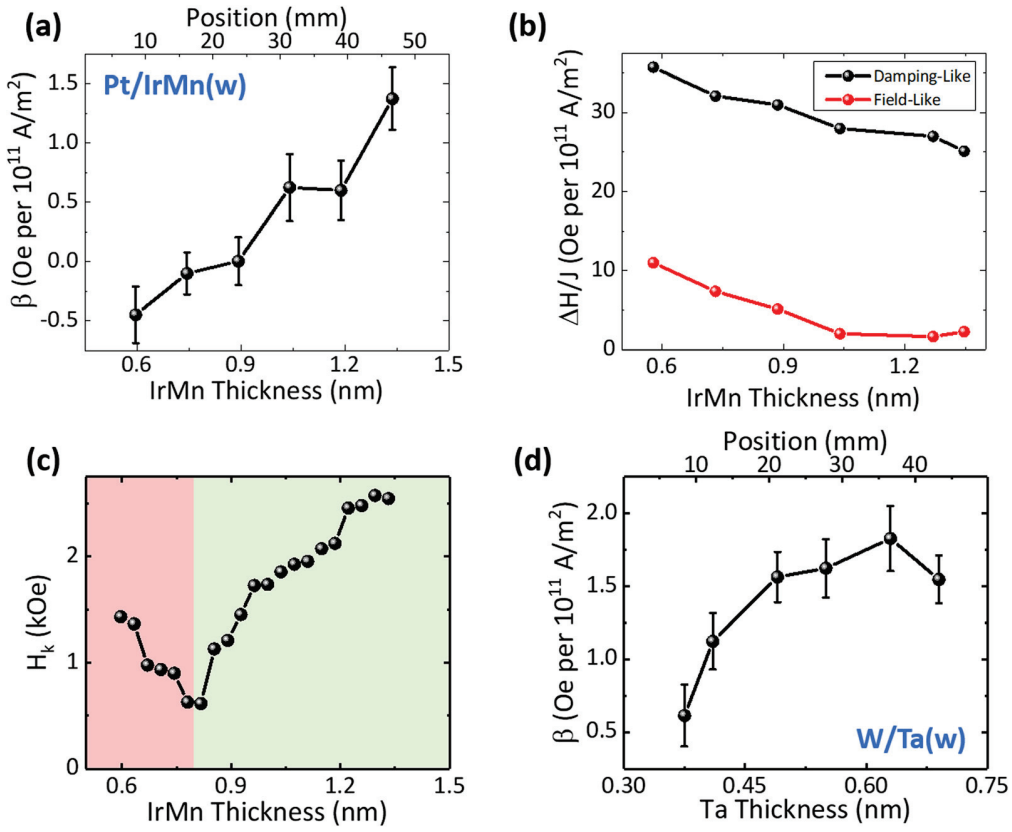

FIG. 3. Characterization of β in Pt/IrMn and W/Ta samples. (a) β as a function of the IrMn thickness in the Pt/IrMn sample. Error bars originate from averaging three different devices and considering the linear fitting errors. (b) Magnitude of damping-like (ΔH_x^{DL}) and field-like (ΔH_y^{FL}) effective SOT fields as a function of IrMn insertion thickness in the Pt/IrMn sample. (c) Effective PMA field (H_k) as a function of IrMn thickness in the Pt/IrMn sample. Two regions with negative (red) and positive (green) slopes are observed. (d) β as a function of Ta insertion thickness in the W/Ta sample.

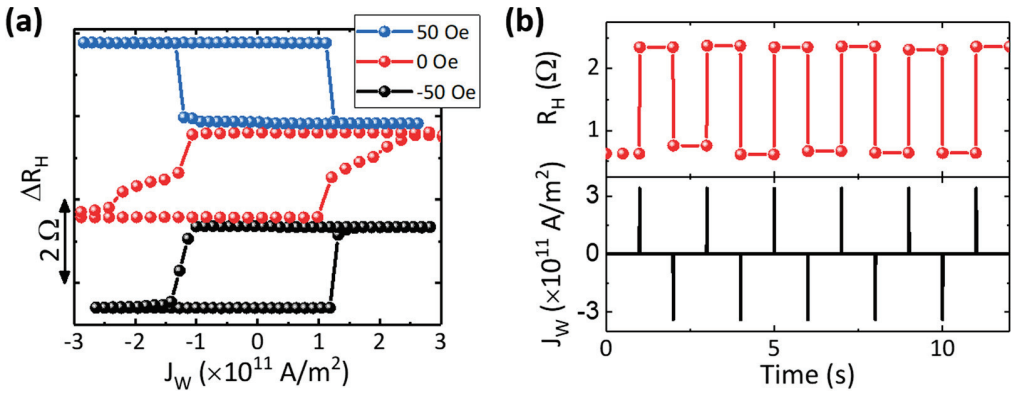

FIG. 4. Deterministic field-free SOT switching of perpendicular magnetization due to H_z^{eff} in the W/IrMn sample. (a) SOT switching under different in-plane magnetic fields, applied along the x axis. ΔR_H is the change in anomalous Hall resistance and J_W is the current density through the W layer. The red curve (0 Oe) shows complete SOT switching without any external magnetic fields. The IrMn insertion thickness in this device is 0.6 nm. (b) Repeatable complete SOT switchings at zero field with successive positive/negative current pulses with a 1 ms duration at a 1 s period.

The important observation is that both the damping-like and field-like effective fields monotonically decrease with the IrMn thickness, which is expected since W and IrMn have opposite signs of the spin Hall angle. We do not see any specific features near 0.8–0.9 nm where the β sign changes. However, we observe a clear correlation between the trends in β and magnetic anisotropy. We extracted the effective PMA fields (H_k) as a function of the IrMn thickness in the Pt/IrMn sample, as shown in Fig. 3(c) (see supplementary material Sec. S6 for more details). We see two different regions in Fig. 3(c); below 0.8 nm, H_k has a negative slope (red) and a negative β, and beyond 0.8 nm, H_k has a positive slope (green) and a positive β. This agreement between the trends of β and H_k is similar to the results of the W/IrMn sample and points to the possible role of chiral symmetry breaking in the creation of H_z^{eff}.[30] Even with the same sign of the spin Hall angle and SOTs, changing the anisotropy gradient's sign results in a change of the SOT-induced spin texture chirality, and consequently, a change of the H_z^{eff} sign (following the discussion in supplementary material Sec. S2). We should add that the magnetization saturation (M_s) has less than 10% variation throughout the length of the Pt/IrMn sample (see Fig. S7 in the supplementary material), which is much smaller than the anisotropy gradient. Furthermore, from the β sign change, we can rule out the role of Oersted fields in the creation of H_z^{eff}.

For both structures presented so far (W/IrMn and Pt/IrMn), we used an asymmetric IrMn insertion layer. To rule out the role of any specific materials such as IrMn, we have also studied H_z^{eff} and β values in the W/Ta material system, where a thin asymmetric insertion of Ta is used to break the symmetry. The results are shown in Fig. 3(d), where a sizable β is observed. We should also point out that in this material system, both the W and Ta have the same sign of the spin Hall angle; nevertheless, we observe a non-zero H_z^{eff} (similar to the Pt/IrMn case).

The direction of H_z^{eff} is locked by the current direction; consequently, each current polarity picks a specific magnetization state ($\pm\hat{z}$), resulting in the field-free deterministic SOT switching, as shown in Fig. 4(a). In the W/IrMn sample, β has a negative slope, i.e., H_z^{eff} points toward $-\hat{z}$ with the current applied along $+\hat{x}$ consistent with the 0 Oe curve in Fig. 4(a). The gradual switching at zero field shows that multiple magnetic domains are created in the intermediate steps and suggests that the switching mechanism is via domain wall nucleation and propagation. The fact that applying in-plane fields of $\pm$50 Oe reverses the switching polarity indicates that in these cases, the switching is determined by the external field.[21] We also studied the repeatability of field-free SOT switching for our samples by applying successive positive/negative current pulses. Figure 4(b) shows the results for the W/IrMn sample, where a complete nonvolatile switching is realized with each current pulse. We should note that in some devices with smaller β values, sometimes the switching is not complete or is reversible, which may be due to the fact that the DMI effective field is not compensated to allow for hysteretic field-free switching.[42]

In summary, we have studied the current-induced effective perpendicular magnetic fields, H_z^{eff}, and conventional SOTs in structures with thin asymmetric dusting layers. Using three different samples with different main heavy-metal/dusting layer materials (W/IrMn, Pt/IrMn, and W/Ta), we show that H_z^{eff} can be generically created in all the structures with lateral asymmetry, independent of the signs of the spin Hall angles, ruling out the role of competing spin currents.[31] Furthermore, we observed a close correlation between the trends in β values and interfacial PMA, showing the importance of interfacial effects in the creation of H_z^{eff} and pointing to the possible role of chiral symmetry breaking.[30] With the help of current-induced H_z^{eff}, we also realized complete field-free deterministic SOT switching of perpendicular magnetization.

See the supplementary material for the correlation between the trends of β values and PMA gradient in the W/IrMn sample, possible role of the chiral symmetry breaking in the induction of H_z^{eff}, absence of H_z^{eff} in a W/IrMn sample with uniform layers, out-of-plane hysteresis loop shifts for the Pt/IrMn sample, spin–orbit torque characterization in the Pt/IrMn sample, extracting the effective PMA fields (H_k) in the Pt/IrMn sample, and the thickness dependence of the magnetization saturation (M_s) in the Pt/IrMn sample.

This work was supported by the NSF under Award Nos. 1935362 and 1909416, the NSF Nanosystems Engineering Research

Center for Translational Applications of Nanoscale Multiferroic Systems (TANMS) with Award No. 1160504, the U.S. Army Research Office MURI program under Grant No. W911NF-16-1-0472, and the Spins and Heat in Nanoscale Electronic Systems (SHINES) Center funded by the U.S. Department of Energy (DOE) under Award No. DE-SC0012670. Guoqiang Yu acknowledges financial support from the National Natural Science Foundation of China (Grant No. 11874409), Beijing Natural Science Foundation (Grant No. Z190009), and K. C. Wong Education Foundation (No. GJTD-2019-14).

DATA AVAILABILITY

The data that support the findings of this study are available from the corresponding author upon reasonable request.

REFERENCES

[1]I. M. Miron, K. Garello, G. Gaudin, P.-J. Zermatten, M. V. Costache, S. Auffret, S. Bandiera, B. Rodmacq, A. Schuhl, and P. Gambardella, "Perpendicular switching of a single ferromagnetic layer induced by in-plane current injection," Nature **476**(7359), 189 (2011).
[2]L. Liu, C.-F. Pai, Y. Li, H. Tseng, D. Ralph, and R. Buhrman, "Spin-torque switching with the giant spin Hall effect of tantalum," Science **336**(6081), 555–558 (2012).
[3]A. Chernyshov, M. Overby, X. Liu, J. K. Furdyna, Y. Lyanda-Geller, and L. P. Rokhinson, "Evidence for reversible control of magnetization in a ferromagnetic material by means of spin–orbit magnetic field," Nat. Phys. **5**, 656 (2009).
[4]L. Berger, "Emission of spin waves by a magnetic multilayer traversed by a current," Phys. Rev. B **54**(13), 9353–9358 (1996).
[5]J. C. Slonczewski, "Current-driven excitation of magnetic multilayers," J. Magn. Magn. Mater. **159**(1), L1–L7 (1996).
[6]E. B. Myers, D. C. Ralph, J. A. Katine, R. N. Louie, and R. A. Buhrman, "Current-induced switching of domains in magnetic multilayer devices," Science **285**(5429), 867 (1999).
[7]K. L. Wang, J. G. Alzate, and P. K. Amiri, "Low-power non-volatile spintronic memory: STT-RAM and beyond," J. Phys. D: Appl. Phys. **46**(7), 074003 (2013).
[8]M. I. Dyakonov and V. I. Perel, "Current-induced spin orientation of electrons in semiconductors," Phys. Lett. A **35**(6), 459–460 (1971).
[9]J. E. Hirsch, "Spin Hall effect," Phys. Rev. Lett. **83**(9), 1834–1837 (1999).
[10]Y. K. Kato, R. C. Myers, A. C. Gossard, and D. D. Awschalom, "Observation of the spin Hall effect in semiconductors," Science **306**(5703), 1910 (2004).
[11]Y. A. Bychkov and É. I. Rashba, "Properties of a 2D electron gas with lifted spectral degeneracy," JETP lett **39**(2), 78 (1984).
[12]V. M. Edelstein, "Spin polarization of conduction electrons induced by electric current in two-dimensional asymmetric electron systems," Solid State Commun. **73**(3), 233–235 (1990).
[13]V. P. Amin and M. D. Stiles, "Spin transport at interfaces with spin-orbit coupling: Formalism," Phys. Rev. B **94**(10), 104419 (2016).
[14]V. P. Amin and M. D. Stiles, "Spin transport at interfaces with spin-orbit coupling: Phenomenology," Phys. Rev. B **94**(10), 104420 (2016).
[15]A. Manchon, J. Železný, I. M. Miron, T. Jungwirth, J. Sinova, A. Thiaville, K. Garello, and P. Gambardella, "Current-induced spin-orbit torques in ferromagnetic and antiferromagnetic systems," Rev. Mod. Phys. **91**(3), 035004 (2019).
[16]C. Safranski, E. A. Montoya, and I. N. Krivorotov, "Spin–orbit torque driven by a planar Hall current," Nat. Nanotechnol. **14**(1), 27–30 (2019).
[17]J. D. Gibbons, D. MacNeill, R. A. Buhrman, and D. C. Ralph, "Reorientable spin direction for spin current produced by the anomalous Hall effect," Phys. Rev. Appl. **9**(6), 064033 (2018).
[18]S. Mangin, D. Ravelosona, J. A. Katine, M. J. Carey, B. D. Terris, and E. E. Fullerton, "Current-induced magnetization reversal in nanopillars with perpendicular anisotropy," Nat. Mater. **5**(3), 210–215 (2006).
[19]S. Ikeda, K. Miura, H. Yamamoto, K. Mizunuma, H. D. Gan, M. Endo, S. Kanai, J. Hayakawa, F. Matsukura, and H. Ohno, "A perpendicular-anisotropy CoFeB–MgO magnetic tunnel junction," Nat. Mater. **9**(9), 721–724 (2010).
[20]G. Yu, P. Upadhyaya, Y. Fan, J. G. Alzate, W. Jiang, K. L. Wong, S. Takei, S. A. Bender, L.-T. Chang, Y. Jiang, M. Lang, J. Tang, Y. Wang, Y. Tserkovnyak, P. K. Amiri, and K. L. Wang, "Switching of perpendicular magnetization by spin–orbit torques in the absence of external magnetic fields," Nat. Nanotechnol. **9**, 548 (2014).
[21]G. Yu, M. Akyol, P. Upadhyaya, X. Li, C. He, Y. Fan, M. Montazeri, J. G. Alzate, M. Lang, K. L. Wong, P. Khalili Amiri, and K. L. Wang, "Competing effect of spin-orbit torque terms on perpendicular magnetization switching in structures with multiple inversion asymmetries," Sci. Rep. **6**, 23956 (2016).
[22]G. Yu, L.-T. Chang, M. Akyol, P. Upadhyaya, C. He, X. Li, K. L. Wong, P. K. Amiri, and K. L. Wang, "Current-driven perpendicular magnetization switching in Ta/CoFeB/[TaOx or MgO/TaOx] films with lateral structural asymmetry," Appl. Phys. Lett. **105**(10), 102411 (2014).
[23]A. Razavi, H. Wu, Q. Shao, C. Fang, B. Dai, K. Wong, X. Han, G. Yu, and K. L. Wang, "Deterministic spin–orbit torque switching by a light-metal insertion," Nano Lett. **20**(5), 3703–3709 (2020).
[24]B. Cui, H. Wu, D. Li, S. A. Razavi, D. Wu, K. L. Wong, M. Chang, M. Gao, Y. Zuo, L. Xi, and K. L. Wang, "Field-free spin–orbit torque switching of perpendicular magnetization by the Rashba interface," ACS Appl. Mater. Interfaces **11**(42), 39369–39375 (2019).
[25]T.-Y. Chen, H.-I. Chan, W.-B. Liao, and C.-F. Pai, "Current-induced spin-orbit torque and field-free switching in Mo-based magnetic heterostructures," Phys. Rev. Appl. **10**(4), 044038 (2018).
[26]S. Fukami, C. Zhang, S. DuttaGupta, A. Kurenkov, and H. Ohno, "Magnetization switching by spin–orbit torque in an antiferromagnet–ferromagnet bilayer system," Nat. Mater. **15**, 535 (2016).
[27]S. A. Razavi, D. Wu, G. Yu, Y.-C. Lau, K. L. Wong, W. Zhu, C. He, Z. Zhang, J. M. D. Coey, P. Stamenov, P. Khalili Amiri, and K. L. Wang, "Joule heating effect on field-free magnetization switching by spin-orbit torque in exchange-biased systems," Phys. Rev. Appl. **7**(2), 024023 (2017).
[28]Y.-W. Oh, S-h Chris Baek, Y. M. Kim, H. Y. Lee, K.-D. Lee, C.-G. Yang, E.-S. Park, K.-S. Lee, K.-W. Kim, G. Go, J.-R. Jeong, B.-C. Min, H.-W. Lee, K.-J. Lee, and B.-G. Park, "Field-free switching of perpendicular magnetization through spin–orbit torque in antiferromagnet/ferromagnet/oxide structures," Nat. Nanotechnol. **11**, 878 (2016).
[29]A. van den Brink, G. Vermijs, A. Solignac, J. Koo, J. T. Kohlhepp, H. J. M. Swagten, and B. Koopmans, "Field-free magnetization reversal by spin-Hall effect and exchange bias," Nat. Commun. **7**, 10854 (2016).
[30]H. Wu, J. Nance, S. A. Razavi, D. Lujan, B. Dai, Y. Liu, H. He, B. Cui, D. Wu, and K. Wong, "Chiral symmetry breaking for deterministic switching of perpendicular magnetization by spin-orbit torque," preprint arXiv:2004.13872 (2020).
[31]Q. Ma, Y. Li, D. B. Gopman, Y. P. Kabanov, R. D. Shull, and C. L. Chien, "Switching a perpendicular ferromagnetic layer by competing spin currents," Phys. Rev. Lett. **120**(11), 117703 (2018).
[32]Y.-C. Lau, D. Betto, K. Rode, J. M. D. Coey, and P. Stamenov, "Spin–orbit torque switching without an external field using interlayer exchange coupling," Nat. Nanotechnol. **11**, 758 (2016).
[33]S-h. C. Baek, V. P. Amin, Y.-W. Oh, G. Go, S.-J. Lee, G.-H. Lee, K.-J. Kim, M. D. Stiles, B.-G. Park, and K.-J. Lee, "Spin currents and spin–orbit torques in ferromagnetic trilayers," Nat. Mater. **17**(6), 509–513 (2018).
[34]K. Cai, M. Yang, H. Ju, S. Wang, Y. Ji, B. Li, K. W. Edmonds, Y. Sheng, B. Zhang, N. Zhang, S. Liu, H. Zheng, and K. Wang, "Electric field control of deterministic current-induced magnetization switching in a hybrid ferromagnetic/ferroelectric structure," Nat. Mater. **16**, 712 (2017).
[35]D. MacNeill, G. M. Stiehl, M. H. D. Guimaraes, R. A. Buhrman, J. Park, and D. C. Ralph, "Control of spin–orbit torques through crystal symmetry in WTe_2/ferromagnet bilayers," Nat. Phys. **13**(3), 300–305 (2017).
[36]H. Wu, S. A. Razavi, Q. Shao, X. Li, K. L. Wong, Y. Liu, G. Yin, and K. L. Wang, "Spin-orbit torque from a ferromagnetic metal," Phys. Rev. B **99**(18), 184403 (2019).
[37]L. You, O. Lee, D. Bhowmik, D. Labanowski, J. Hong, J. Bokor, and S. Salahuddin, "Switching of perpendicularly polarized nanomagnets with spin orbit torque without an external magnetic field by engineering a tilted anisotropy," Proc. Natl. Acad. Sci. U. S. A. **112**(33), 10310 (2015).

[38]C. He, S. A. Razavi, G. Yu, X. Ma, H. Wu, Q. Shao, K. L. Wong, S. Shen, Y. Zhao, Y. Pei, Q. Chen, X. Li, S. Wang, and K. L. Wang, "Study of the perpendicular magnetic anisotropy, spin–orbit torque, and Dzyaloshinskii–Moriya interaction in the heavy metal/CoFeB bilayers with $Ir_{22}Mn_{78}$ insertion," Appl. Phys. Lett. **116**(24), 242407 (2020).
[39]K. Garello, I. M. Miron, C. O. Avci, F. Freimuth, Y. Mokrousov, S. Blügel, S. Auffret, O. Boulle, G. Gaudin, and P. Gambardella, "Symmetry and magnitude of spin–orbit torques in ferromagnetic heterostructures," Nat. Nanotechnol. **8**, 587 (2013).
[40]A. Barranco, A. Borras, A. R. Gonzalez-Elipe, and A. Palmero, "Perspectives on oblique angle deposition of thin films: From fundamentals to devices," Prog. Mater. Sci. **76**, 59–153 (2016).
[41]D. Wu, G. Yu, C.-T. Chen, S. A. Razavi, Q. Shao, X. Li, B. Zhao, K. L. Wong, C. He, Z. Zhang, P. K. Amiri, and K. L. Wang, "Spin-orbit torques in perpendicularly magnetized $Ir_{22}Mn_{78}/Co_{20}Fe_{60}B_{20}/MgO$ multilayer," Appl. Phys. Lett. **109**(22), 222401 (2016).
[42]J. Yu, X. Qiu, Y. Wu, J. Yoon, P. Deorani, J. M. Besbas, A. Manchon, and H. Yang, "Spin orbit torques and Dzyaloshinskii-Moriya interaction in dual-interfaced Co–Ni multilayers," Sci. Rep. **6**(1), 32629 (2016).